Journal of
Applied Crystallography
ISSN 0021-8898

Received 16 August 2006
Accepted 22 November 2006

Current status of the 40 m small-angle neutron scattering instrument development at the HANARO research reactor

Young-Soo Han,[a]* Sung-Min Choi,[b] Tae-Hwan Kim,[b] Chang-Hee Lee[a] and Hark-Rho Kim[a]

[a]Korea Atomic Energy Research Institute, PO Box 105, Yuseong, Daejeon, Republic of Korea, and [b]Department of Nuclear and Quantum Engineering, Korea Advanced Institute of Science and Technology, 373-1, Guseong-dong, Yuseong, Daejeon, Republic of Korea. Correspondence e-mail: yshan@kaeri.re.kr

The cold neutron research facility project at the Korean HANARO research reactor was launched in 2003. A state-of-the-art small-angle neutron scattering instrument was selected as a top-priority instrument. An analytical calculation was used to obtain the optimum instrument design and the appropriate range of scattering vectors of the instrument. Then, in order to optimize the instrument layout and to enhance the instrument's performance, a Monte Carlo simulation was performed. The Q range [where Q is the magnitude of the scattering vector given by $(4\pi/\lambda)\sin(\theta/2)$, θ is the scattering angle and λ is the wavelength] of the instrument will extend from 0.0008 to 1.0 Å^{-1}. The instrument layout was optimized based on simulation results. The maximum flux at the sample position can reach about 5.5×10^{7} n cm^{-2} s^{-1}.

1. Introduction

The 30 MW HANARO research reactor at the Korea Atomic Energy Research Institute (KAERI) is a world class research reactor which has a peak thermal neutron flux of 5.4×10^{14} n cm^{-2} s^{-1}. However, as it does not have a cold neutron source and cold neutron instruments, the potential impact of HANARO on the scientific and engineering research areas in Korea has not been fully exploited yet. The cold neutron research facility project was launched in July 2003. A state-of-the-art small-angle neutron scattering (SANS) instrument was selected as a top-priority instrument by an instrument selection committee which consisted of domestic users and HANARO personnel.

Since neutron instruments are very expensive to construct, it is essential to optimize the designs by simulations. Currently several Monte Carlo simulation tools for neutron instruments are available. Monte Carlo simulations are being used for new instrument and guide designs (Bordallo *et al.*, 2002; Demmel *et al.*, 2004; Lieutenant *et al.*, 2005; Tamura *et al.*, 2004; Zeitelhack *et al.*, 2006). Recently, a study to compare the various simulation tools showed that the level of agreement between these programs is fairly good for the triple-axis spectrometer H8 at Brookhaven National Laboratory, which was chosen as a sample instrument (Seeger *et al.*, 2002).

An analytical calculation was applied to obtain the optimum SANS instrument design and the appropriate scattering vector range of the instrument. Then, in order to optimize the instrument layout and to enhance the instrument performance, a Monte Carlo simulation was performed.

2. Analytical calculation

The Q range [where Q is the modulus of the scattering vector defined by $(4\pi/\lambda)\sin(\theta/2)$, θ is the scattering angle and λ is the wavelength] of the SANS instrument at HANARO is estimated from a simple calculation. In this calculation, both the length of the pre-sample flight path and the maximum sample to detector distance are assumed to be 20 m, comprising a 40 m SANS instrument. All the configurations are set to be symmetric; the source to sample distance (L1) and the sample to detector distance (L2) are equal. For all the configurations except when L1 = L2 = 20 m, the source aperture and the sample aperture are assumed to be 5 cm (A1) and 1.25 cm (A2) in diameter respectively. For the highest collimation (L1 = L2 = 20 m), a source aperture of 3 cm is used.

The minimum Q can be calculated easily by using the beam size at the detector, the detector resolution (d = 0.5 cm) and the sample to detector distance. For simplicity, the beam stop in front of the detector is assumed to vary continuously and vertical spreading of the beam due to gravity is ignored. The beam diameter B at the detector is simply given as

$$\mathrm{B} = (\mathrm{L2}/\mathrm{L1})(\mathrm{A1} + \mathrm{A2}) + \mathrm{A2} \quad (1)$$

and the minimum detectable scattering angle $\theta_{\min}$ is

$$\theta_{\min} = \tan^{-1}\left(\frac{\mathrm{B}/2 + d}{\mathrm{L2}}\right). \quad (2)$$

Then, the minimum Q can be calculated by using

$$Q_{\min} = (4\pi/\lambda)\sin(\theta_{\min}/2). \quad (3)$$

To calculate the maximum Q, a detector offset of 45 cm is assumed and the maximum detectable scattering angle $\theta_{\max}$ is obtained from the corner edge of the detector.

The calculated Q ranges of the 40 m SANS instrument with different configurations are given in Fig. 1. The accessible Q ranges are 0.0019–1.00 Å^{-1} for 5 Å, 0.0013–0.71 Å^{-1} for 7 Å, and 0.0010–0.557 Å^{-1} for 9 Å. It should be noted that the entire Q range for a given neutron wavelength can be accessed by only two instrument configurations (L1 = L2 = 20 m and L1 = L2 = 1 m), which is made possible by the wide dynamic range of a large detector (1 m × 1 m).

Table 1
The parameters used in the simulation.

Section	Length (m)	Cross section (cm × cm)	Coating material	Comments
G1	4.8	5 × 5	$m = 2$	Straight guide, distance from source = 1.84 m
G2	Variable	5 × 5	$m = 2$	Curved guide, radius of curvature variable
G3	20	5 × 5	Ni-58, Ni-natural, $m = 2$	Straight guide
RG	0, 4, 8, 12, 16, 18	5 × 5	Ni-58, Ni-natural, $m = 2$	Removable, straight guides
L1	2, 4, 8, 12, 16, 20	—	—	Source to sample distance

When the effects of gravity are included, the beam size in the vertical direction will increase due to wavelength spreading and the minimum Q, especially for long wavelength neutrons, will also increase. However, by using anti-gravity prisms at the expense of a certain beam attenuation, the effects of gravity can be corrected. Furthermore, by using refractive focusing lenses, the minimum Q can be decreased further and a minimum Q of 0.0008 Å^{-1} or less is achievable (Choi *et al.*, 2000).

3. Simulation

The characteristics of the SANS instrument were simulated by using *Virtual Instrumentation Tool for ESS* (*VITESS*) (http://www.hmi.de/projects/ess/vitess/). The configurations of the guides and the SANS instrument used in the simulations are shown in Table 1. The guide G1 is an inpile straight guide with a fixed length and G2 is a curved guide. G3 is the second straight guide before the velocity selector. RG are removable guide sections and L1 is the distance between the source aperture and the sample aperture. The length of RG + L1 of 20 m is fixed.

Based on the MCNP (Monte Carlo *N* particle) simulation results, the neutron spectrum of the cold source is assumed to be a two-temperature distribution of 26.3 K with a total integrated flux of 7.7 × 10^{12} n cm^{-2} s^{-1} and of 125.2 K with a total integrated flux of 6.4 × 10^{13} n cm^{-2} s^{-1}. The neutron spectrum at the entrance of G1, which is 1.84 m away from the cold neutron source, is shown in Fig. 2.

The neutron spectra after guides G1, G2 and G3 are also shown in Fig. 2. In this calculation, it was assumed that the G1 and G2 guides were made of $m = 2$ supermirrors and the G3 guide was made of natural Ni. As the neutron beam passes through each guide section, the beam intensity drops over the entire wavelength.

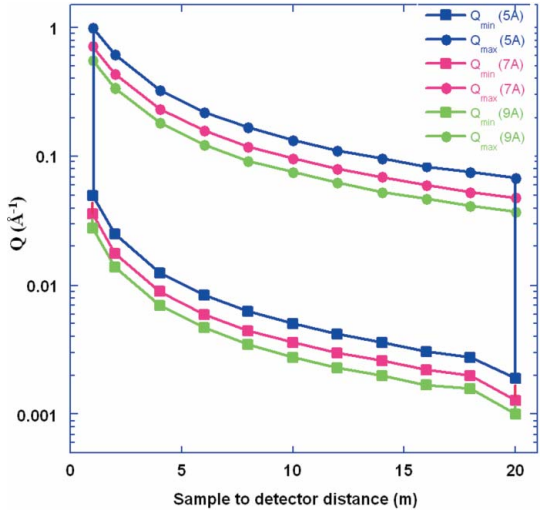

Figure 1
Q range of the 40 m SANS instrument for different configurations.

The neutron spectra when different coating materials (Ni-58, Ni-natural, $m = 2$ supermirror) are used for G3 are shown in Fig. 3. Here, the $m = 2$ supermirror was assumed for G1 and G2. The intensity is

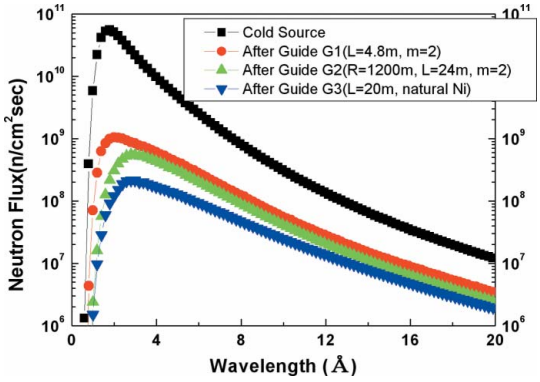

Figure 2
The neutron spectra at the cold source and after guides G1, G2 and G3.

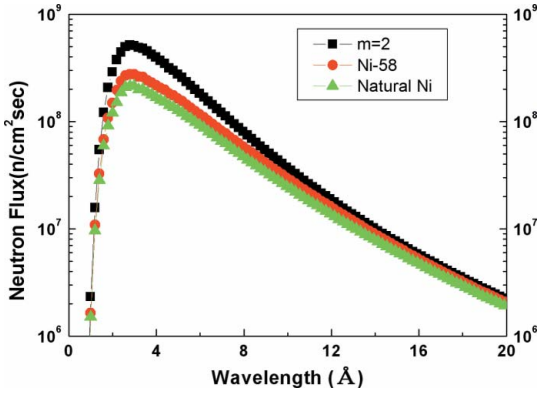

Figure 3
The neutron spectra right after guide G3 when guide G3 uses different coating materials ($m = 2$, Ni-58 and Ni-natural) and G1 and G2 use an $m = 2$ supermirror.

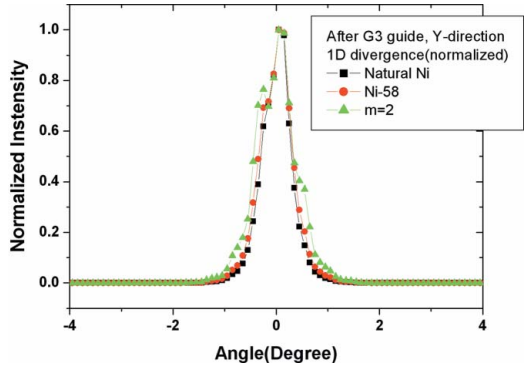

Figure 4
The beam divergences right after guide G3 when G1 and G2 use an $m = 2$ supermirror and G3 uses different coating materials ($m = 2$, Ni-58 and Ni-natural).

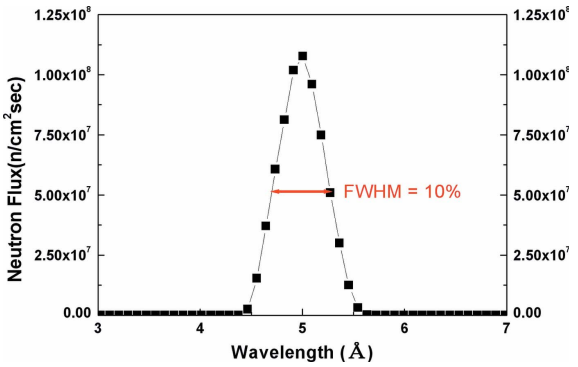

Figure 5
The neutron wavelength distribution after the velocity selector.

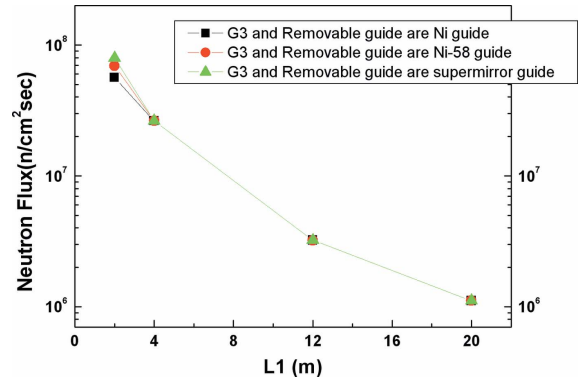

Figure 6
The neutron intensity on the sample for different source to sample distances with different guide coating materials.

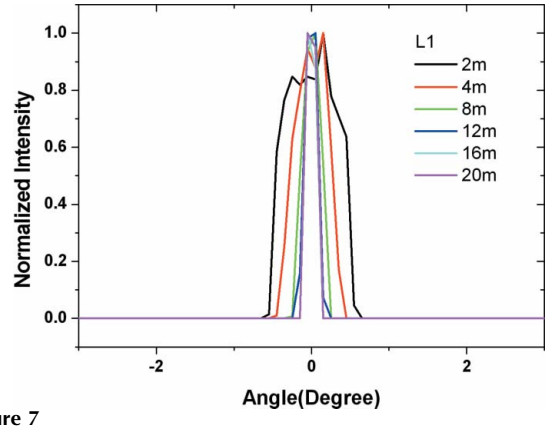

Figure 7
The beam divergence for different source to sample distances L1. A1 = 5.0 cm and A2 = 1.25 cm.

highest when the $m = 2$ supermirror is used, followed by Ni-58 and Ni-natural as expected. The higher intensity of G3 with the $m = 2$ supermirror is simply due to its larger angular divergence, as can be seen in Fig. 4. However, since the beam divergences required for a high or medium resolution of the SANS configurations are much tighter than that of the $m = 2$ supermirror, the intensity gain of the $m = 2$ supermirror over the others will not be fully utilized.

We used the simulation parameters for the velocity selector obtained from the Astrium neutron velocity selector. The relationship between the selector speed U (r.p.m.) and the neutron wavelength λ is expressed as λ [Å] $= A + B/U$ [r.p.m.], with $A = 0.11832$ and $B = 124\,270$ for the Astrium neutron velocity selector. Following this relation, the rotation speed of the selector is set to provide neutrons of wavelength 5 Å. After that, a neutron spectrum with a peak wavelength of 5 Å is obtained as shown in Fig. 5. In accordance with the manufacturer's specifications, the wavelength distribution (full width at half maximum) is also obtained as 10%.

For neutrons of a wavelength of 5 Å, the neutron intensities on a sample with different lengths (0, 8 and 18 m) of the removable guide RG, *i.e.* different source to sample distances L1 (20, 12 and 2 m), were calculated. A source aperture A1 of 5 cm and a sample aperture A2 of 1.25 cm in diameter were used in all cases. This calculation was repeated with different coating materials (Ni-58, Ni-natural, $m = 2$ supermirror) for guides G3 and RG. The $m = 2$ supermirrors are used for guides G1 and G2 in all cases. As can be seen in Fig. 6, the intensity increases as L1 decreases, *i.e.* more removable guides are inserted. The difference between the different coating materials for G3 and RG is almost negligible for L1 = 20, 8 and 4 m, and it shows only when L1 = 2 m. Therefore, compared to Ni-58 or Ni-natural there is no advantage in using the $m = 2$ supermirror for G3 and RG when high or medium resolution SANS configurations are used. This can be understood from the beam divergence of these configurations shown in Fig. 7.

In order to optimize the location of the 40 m SANS instrument in the guide hall, the simulations were performed with various radii of curvature for the G2 guide with a fixed length and the results are shown in Fig. 8. The neutron intensity after the G2 guide increases

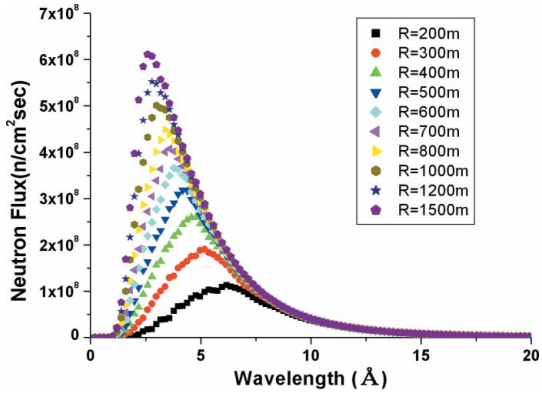

Figure 8
The neutron flux after the G2 guide with various radii of curvature for the G2 guide at a fixed length of 24 m.

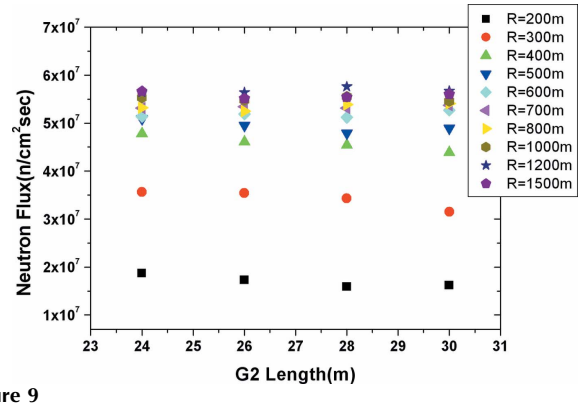

Figure 9
The neutron flux at the sample position with various radii of curvature and lengths of the G2 guide at a selected wavelength of 5 Å (G2 + G3 = 36 m, L1 = 2 m).

and the peak wavelength is shifted to a lower wavelength with an increase in the radius of curvature. Fig. 9 shows the flux at the sample position with various radii of curvature and lengths of the G2 guide at the selected wavelength of 5 Å. In these simulations, the length of G2 + G3 is fixed as 36 m by considering the location of the SANS instrument in the guide hall. The flux at the sample position increases with the radius of curvature of the G2 guide up to 600 m and it is saturated above the radius of curvature of the G2 guide of 600 m. This result shows that the location of the 40 m SANS instrument can be adjusted by satisfying the radius of curvature of the curved guide above 600 m with a length of the curved guide from 26 to 32 m.

The location of the 40 m SANS instrument starting point in the guide hall is dependent on the radius of curvature and the length of the G2 and G3 guides. The same location can be realized with a wide range of radius of curvature of 200–3000 m by adjusting the length of the G2 and G3 guides. For example, both conditions of G2 = 6 m, G3 = 30 m and the radius of curvature = 400 m and the conditions of G2 = 24 m, G3 = 12 m and the radius of curvature = 1200 m have the same location in the guide hall. Simulations were performed in order to compare the conditions with the different radius of curvature and length of the G2 and G3 guides with the same locations in the guide hall.

Fig. 10 shows the neutron flux at the sample position with various radii of curvature of the G2 guide. In these simulations, the length of G2 + G3 is fixed as 36 m with L1 = 2 m. The neutron flux is independent of the radius of curvature and it fluctuates within a range of 10% as shown in Fig. 10. This result is considered to be because the neutron flux is affected not by the radius of curvature but by the optimum reflection at the curved guide exit in these simulation conditions.

Fig. 11 shows the simulated neutron flux at the sample position (n cm^{-2} s^{-1}) for wavelengths in the range 5–9 Å with various collimation distances. The radius of curvature and the length of the G2 guide are 800 m and 24 m, respectively. The length of the G3 guide is 12 m. A source aperture A1 of 5 cm and a sample aperture A2 of 1.25 cm in diameter were used. The simulated flux values shown in Fig. 11 are about 50% of the measured flux of the ILL D22 SANS instruments at the same wavelength of 5 Å and the same collimation length of 2 m (http://www.ill.fr/YellowBook/D22). The thermal power of the HANARO reactor is half that of the ILL one. The neutron flux above 3 Å at the ILL cold source is 8×10^{14} n cm^{-2} s^{-1} (http://www.ill.fr/YellowBook/D22), while the calculated neutron flux at the HANARO cold source is 2×10^{13} n cm^{-2} s^{-1}. If only the thermal power of the two reactors is considered, our results give us a reliable approximation of the performance of the designed instrument. Concerning the flux at the cold source of the two reactors, even though the real incident flux at the sample position would be affected by several factors, it is considered that the optimum guide design based on the simulation result provides us with better performance of our instrument.

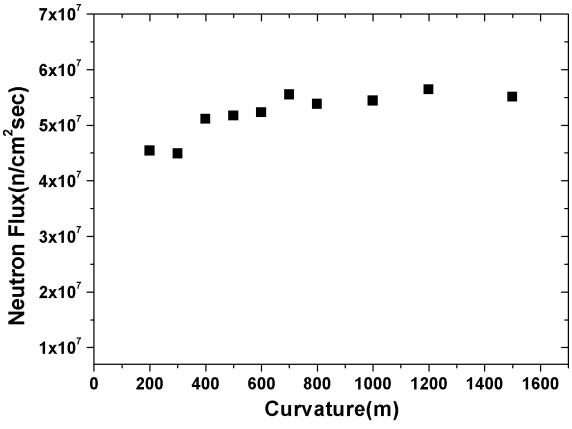

Figure 10
The neutron flux at the sample position with various radii of curvature at the selected wavelength of 5 Å (G2 + G3 = 36 m, L1 = 2 m).

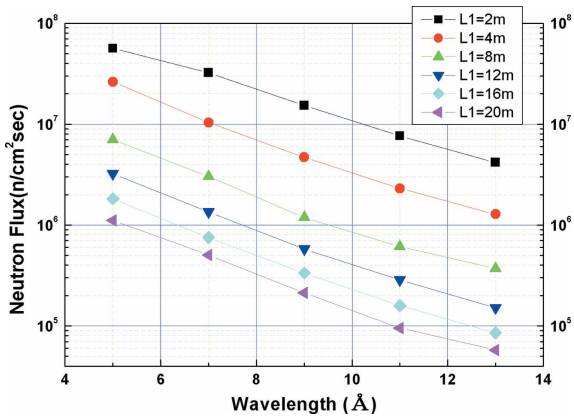

Figure 11
The simulated neutron flux at the sample position (n cm^{-2} s^{-1}) for collimation distances in the range 2–20 m with various wavelengths. The radius of curvature and the length of the G2 guide are 1200 and 24 m, respectively. A source aperture A1 of 5 cm and a sample aperture A2 of 1.25 cm in diameter were used.

By performing additional simulations with several conditions, the following results were obtained:

(1) The intensity at the exit of guide G2 is shifted to one side since a curved guide is used for G2, but when the neutrons pass through guide G3 the beam intensity distribution becomes uniform. To obtain a uniform distribution, at least 10 m for guide G3 is required.

(2) The cross section of the inpile guide is 5 cm × 15 cm (W × H). Because the SANS instrument uses a guide with a cross section of 5 cm × 5 cm (W × H), its position can be selected by installing the G2 guide. When comparing the flux at the sample with the G2 guide position, the flux at the centre part is 7–9% higher than that at the top or bottom part.

The radius of curvature of the G2 guide should exceed 700 m and at least 10 m in length for the G3 guide is required. If the guide before the instrument fulfils these two conditions, optimum flux and beam uniformity can be achieved.

4. Conclusions

An analytical calculation was used to obtain the optimum SANS instrument design and the Q range of the instrument. Then, in order to optimize the instrument layout and to enhance the instrument performance, a Monte Carlo simulation was performed. The Q range of the instrument will cover from 0.0008 to 1.0 $Å^{-1}$. The instrument layout was optimized based on the simulation results. The maximum flux at a sample position can reach about 5.5×10^{7} n cm^{-2} s^{-1}.

This work has been carried out under the Nuclear R & D Program of the Ministry of Science and Technology.

References

Bordallo, H. N., Herwig, K. W. & Zsigmond, G. (2002). *Nucl. Instrum. Methods Phys. Res. A*, **491**, 216–225.

Choi, S. M., Barker, J. G., Glinka C. J., Cheng, Y. T. & Gammel, P. L. (2000). *J. Appl. Cryst.* **33**, 793–796.
Demmel, F., de Geuser, F. & Rival, P. (2004). *Physica B*, **350**, e695–e697.
Lieutenant, K., Gutberlet, T., Wiedenmann, A. & Mezei, F. (2005). *Nucl. Instrum. Methods Phys. Res. A*, **553**, 592–603.
Seeger, P. A., Daemon, L. L., Farhi, E., Lee, W. T., Wang, X. L., Passell, L., Saroun, J. & Zsigmond, G. (2002). *Neutron News*, **13**, 24–29.
Tamura, I., Suzuki, M., Hazawa, T., Moriai, A., Hori, N., Sasajima, F. & Soyama, K. (2004). *Nucl. Instrum. Methods Phys. Res. A*, **529**, 234–237.
Zeitelhack, K., Schanzer, C., Kastenmüller, A., Röhrmoser, A., Daniel, C., Franke, J., Gutsmiedl, E., Kudryashov, V., Maier, D., Päthe, D., Petry, W., Schöffel, T., Schreckenbach, K., Urban, A. & Wildgruber, U. (2006). *Nucl. Instrum. Methods Phys. Res. A*, **560**, 444–453.